RECENT RESULTS: COLLIDER DETECTOR AT FERMILAB

The CDF Collaboration[*]

Presented by Virgil E. BARNES

Purdue University, West Lafayette, Indiana 47907

The status and prospects of the 1988-89 CDF data taking run with $\bar{p}p$ collisions at 1.8 TeV, are briefly reviewed. Results are presented on minimum-bias inelastic events from 1987 data at 1.8 and 0.63 TeV center of mass energy, and are compared with data at lower energy and with data from the C0 experiment Transverse momentum spectra harden as the center of mass energy $\sqrt{s}$ increases. Charged particle density in rapidity, and mean transverse momentum, increase faster than ln(s). Charged particles frequently form jet-like clusters with transverse energy of a few GeV. The present CDF data do not permit conclusions for or against the possible formation of a quark gluon plasma.

1. INTRODUCTION

The Collider Detector at Fermilab is a large, general purpose azimuthally symmetric $\sim 4\pi$ detector covering polar angles from $2°$ to $178°$ with respect to the collision axis, corresponding to a range of pseudorapidity $-4 < \eta < 4$ $[\eta = \ln(\tan(\theta/2))]$. CDF has high resolution tracking in a ~ 1.5 T magnetic field followed by fine-grained projective tower calorimeters, and then by muon tracking over portions of the above range of η. The detector has been described in detail elsewhere[1]. It is well suited to studying individual charged hadrons, jets, and leptons having a wide range of energies and transverse momenta.

In Section 2, the potential of CDF for studying hard collision processes, production of heavy particles, quark compositeness, and minimum bias inelastic events will be discussed in the context of the ongoing high-statistics data run. Sections 3 and 4 discuss central portions of the detector, and the trigger and event selection for minimum bias events recorded in the first CDF physics run, in 1987. Data will include: (Sect. 5) charged particle multiplicities, N, and rapidity density, $dN/d\eta$, (6) charged particle p_T spectra, mean p_T, and $< p_T >$ vs N, (7) the p_T spectra of K_s^0, and (8) charged particle correlations and clustering.

2. STATUS AND PROSPECTS OF THE 1988-89 RUN

In September, 1988 the TeVatron collider reached and exceeded the design luminosity of 1.0×10^{30} cm^{-2} sec^{-1} in several 6×6 bunch $p\bar{p}$ stores at 1.8 TeV. By the end of the month the collider had delivered over 1 pb^{-1} of time-integrated luminosity to CDF in the B0 collision area, and the average rate had risen to ~ 1 pb^{-1}/month. This extrapolates to 8 pb^{-1} delivered by the end of the run on April 30, 1989. [By November 1, CDF had recorded on magnetic tape over 770 nb^{-1} of data, and was utilizing the delivered luminosity with good efficiency.] The present goal is to have a data sample greater than 3 pb^{-1} for 1988-89.

---

[*] ANL-Brandeis-University of Chicago- Fermilab-INFN, Frascati-Harvard-University of Illinois-KEK-LBL-University of Pennsylvania-INFN, University and Scuole Normale, Pisa-Purdue- Rockefeller-Rutgers-Texas A&M-Tsukuba-University of Wisconsin

At the design luminosity, the event rate seen by the minimum bias inelastic event trigger is 44 kHz. About 1.5 events per second are selected to be written to tape. A Fastbus-based Level 2 hardware trigger system, followed by a software Level 3 trigger using a 30-node ACP computer farm, accepts more than one dozen trigger categories designed to select electrons or muons with large p_T, dilepton events, high p_T hadronic jets or multiple jets, and events with large missing transverse energy signalling the presence of a neutrino or some other neutral non-interacting particle.

Among a few highlights of the potential of the present run are:

A.) More than 3000 $W^{\pm} \rightarrow e\nu$ events and more than 300 $Z \rightarrow e^+e^-$ events, where an electron is seen in the central calorimeters. This is a substantial increase in the world sample of W and Z. The Standard Model predicts[2] (and CDF observed in the 33nb^{-1} data run in 1987)[3] a W production cross section at 1.8 TeV ~3.6 (4.6) times greater than at 630 GeV.

B.) Although particle production cross sections drop rapidly with increasing particle mass, there is a substantial cross section advantage at 1.8 TeV compared to, say, 630 GeV. This advantage increases with particle mass[4], and is a factor of order 100 for particles with 300 GeV/c^2 mass. CDF will be able either to observe, or else set mass limits on, hypothetical new Z' and W' bosons up to masses of 400 and 500 GeV/c^2, respectively. In general, searches for new heavy particles predicted, for example, by Supersymmetry or Technicolor theories, or for the Higgs particle, should have sensitivity up to several hundred GeV masses.

C.) Some 100 $t\bar{t}$ pairs would be produced[4] if the top quark mass is 110 GeV/c^2. The dominant decay mode would be $t \rightarrow b + W$, with 34% probability that one of the Ws would decay to $e\nu$ or $\mu\nu$, modes for which standard model backgrounds to the top signal are less severe. It is estimated that CDF may be sensitive to the top quark up to about 100 GeV mass in the present run.

D.) The Jet p_T spectrum will be studied well beyond 300 GeV/c, further improving tests of QCD and/or probing for quark compositeness beyond the limit $\Lambda_c > 700$ GeV established from the 1987 CDF data[5].

E.) A small number of $J/\psi \rightarrow \mu^+\mu^-$ have been seen in jet trigger events from the 1987 run. A low-mass dimuon trigger in the 1988 run is hoped to accept some J/ψ.

F.) Once substantial integrated luminosity has been acquired for hard collisions, it is hoped to extend the study of minimum bias processes in a variety of ways: (a) implement a Level 3 trigger for high charged particle multiplicities; (b) a Level 3 trigger for decays of neutral strange particles to two charged particles; (c) run with a series of jet triggers having relatively low thresholds in ΣE_T (scalar sum of calorimeter energies weighted by $sin(\theta)$), ranging from 5 to 25 GeV/c; (d) runs at lower $\sqrt{s}$, such as 630 and 1100 GeV; (e) study of elastic and single diffractive dissociation events using the small-angle forward detectors consisting of Silicon microstrip detectors and drift chambers mounted in Roman pots; and (f) runs at somewhat reduced magnetic field to extend the charged particle p_T spectrum below 400 MeV/c.

3. THE CENTRAL TRACKING DETECTORS

The present minimum bias data analysis uses charged tracks found in the Vertex Time Projection Chamber (VTPC)[6] or in the Central Track Chamber (CTC)[7] (Fig. 1).

The VTPC covers a range $|\eta| < 3.5$, with full acceptance for $|\eta| < 3.0$. It consists of 8 modules each 30 cm long in Z and 22 cm in radius, with 15 cm drift distance in each

half cell. There are 3072 sense wires which lie on the chords of circles centered on the collision axis. Sense wires are arranged in octants. Azimuthal coverage is complete. Tracks are reconstructed in the R-Z (non-bending) direction, with resolution $\sigma \sim$ 200 to 500 μm (depending on θ) and two-track resolution 6 mm at $\theta = 90°$. Cathode pads installed on some modules provide limited R-ϕ tracking, but those data were not used in the present analysis.
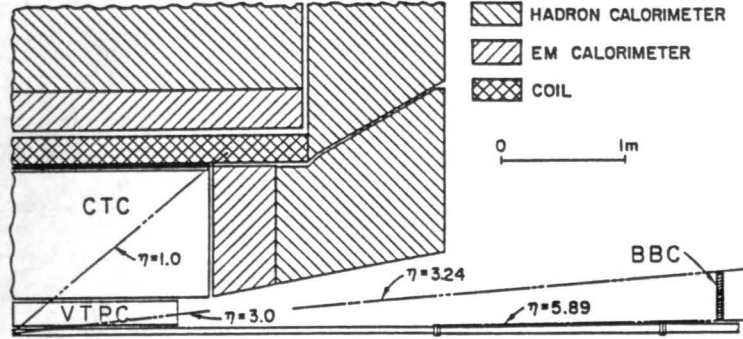

Fig. 1 Sectional view of one-quarter of the central portion of the CDF detector.

The CTC is a large drift chamber with inner radius 0.3 m and outer radius 1.3 m. Sense wires are arranged in 5 axial superlayers of 12 layers each, and 4 small-angle stereo ($\pm 3°$) superlayers of 6 layers each, providing full 3-dimensional reconstruction for $|\eta| < \sim$ 1.3. Coverage is complete in azimuth. The transverse momentum resolution, including both single hit resolution and multiple scattering, was $\sigma_{p_T}/p_T^2 \leq 0.003$ GeV^{-1} for $|\eta| \leq 1.0$. The CTC data permit reconstruction of over 100 tracks in events with high local track density.

4. TRIGGER AND EVENT SELECTION

Scintillator hodoscopes located at Z (along the beam) $= \pm$ 5.82 m and covering the range 3.24 $< |\eta| <$5.89 (the Beam-Beam Counters or BBC) are used to trigger on most of the inelastic cross section, and also serve as a luminosity monitor.

The minimum bias (MB) data samples were obtained with a trigger requiring that at least one charged particle traverse each set of BBC, in coincidence with the beam crossing. At 1.8 TeV (630 GeV), 55,700 (9,400) triggers were analyzed. Beam-beam collision events were selected by requiring that (a) at least 4 charged particles were found in the VTPC in the range -3$< \eta <$ 3 and at least one of these tracks be in each hemisphere ($\eta > 0$ and $\eta < 0$), and (b) the Z of the vertex from BBC timing agreed within 16 cm with Z_{VTPC} determined from VTPC tracks.

The Beam-Beam event vertices were distributed gaussianly in Z with a typical σ_z of 40 cm. To ensure uniform VTPC track acceptance, we also required $|Z_{VTPC}| < 65$ cm. After these cuts, the contamination of non-beam-beam events was estimated to be less than 2.5% in the single low-luminosity 630 GeV run, and less than 0.5% at 1.8 TeV, where the typical luminosity was up to 4 $\times$ 10^{28} cm^{-2}sec^{-1} for MB runs. The final MB sample consists of 51,000 (4,800) events at the two energies.

The effective BBC trigger cross section was estimated by extrapolating the total and elastic cross sections to 1.8 TeV, giving 75 mb and 15 mb, respectively. The 60 mb of

3

inelastic cross section is divided into single diffractive (SD), double diffractive (DD), and non diffractive (ND) events. The acceptances (ϵ) of the BBC were found by Monte Carlo simulation and are tabulated below:

$\sqrt{s}$(TeV)	ϵ: ND	DD	SD;	σ_{eff}(mb)
1.8	96%	57%	16%	43±6
0.63	93%	57%	11%	34±3

A recent UA4 measurement[8] of $\sigma_{SD} = 9.4 \pm 0.7$ mb at 546 GeV lowers the estimates of σ_{ND} and hence lowers both σ_{eff} estimates. Since σ_{DD} is a few mb, the CDF MB sample is dominantly non-diffractive inelastic events.

5. CHARGED PARTICLES: MULTIPLICITY AND DENSITY

The VTPC counts particles with good efficiency up to $\eta = 3$. A correction has been applied for geometrical acceptance as a function of η and of Z of the vertex. Several necessary corrections have not yet been applied: (a) tracks with p_T below 50 MeV/c will not traverse the full radius of the VTPC, and will spiral along Z, resulting in a 5 - 10% inefficiency; (b) particle decays, photon conversions, and secondary interactions can add particles which pass the 5σ vertex-pointing cut, a 10 - 15% effect; (c) recent studies involving Monte Carlo event simulation and track reconstruction, and human scanning with interactive track reconstruction, indicate that track reconstruction inefficiencies and errors are 3 - 5%.

We estimate that without the above corrections, the overall error (η-dependent) is ~10% or less. These errors are largely common to the 1.8TeV and 630 GeV data and should cancel when taking ratios.
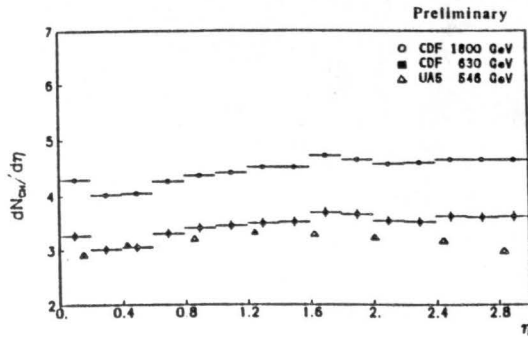

Fig. 2 $dN/d\eta$ vs. η for CDF data at 0.63 and 1.8 TeV, and for UA5 data at 0.546 TeV.
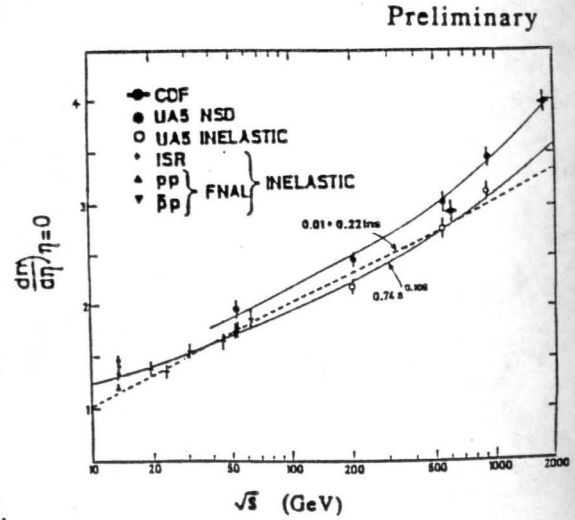

Fig. 3 $dN/d\eta|_{\eta=0}$ vs. $\sqrt{s}$.

The charged particle pseudorapidity distributions at our two energies are shown in Fig. 2, together with the UA5 data[9]. The data, which are folded about $\eta=0$, all form plateaus over six units of η. The value of $dN/d\eta|_{\eta=0}$ is $1.33 \pm .04$ times larger at 1.8 TeV than at 630

4

GeV. The quoted error does not include the 10% systematic error common to both energies. The ratio of pleateau heights averaged over the range $|\eta| < 1$ is, on a similar basis, 1.27 ± .04. This will be used in the next section in deriving $< p_T >$. These ratios are slightly higher than the value 1.22 - 1.25 predicted by the Dual Parton Model[10], or the value 1.20 predicted by the Lund-PYTHIA Monte Carlo program[11].

Fig. 3 shows the values of $dN/d\eta|_{\eta=0}$ as a function of $\sqrt{s}$. Good fits to the UA5 non-single-diffractive data and to the present CDF data (which are approximately an NSD sample) are obtained with either of the following s dependences:

$0.843\ s^{0.102}$	$\chi^2 = 5.4$ for 4 degrees of freedom
$1.129 + 0.0122\ \ln^2(s)$	$\chi^2 = 6.1$ for 4 DOF

The two fits, which are shown as the top curve, are almost indistinguishable, and differ by at most 1.5% over the range of the fit. The power law fit has essentially the same s dependence as the earlier fit to total inelastic data at lower energies. The plateau clearly rises faster than ln(s).

Fig. 4 shows charged particle multiplicity distributions in terms of the Koba-Nielsen-Olesen (KNO) variables $< N > P(N) = \psi(N/< N >)$, where $P(N) = \sigma(N)/\sigma_{inelastic}$. KNO scaling states that ψ is independent of s. Scaling works fairly well at low s and is clearly broken[12] between ISR energies ($\sqrt{s} \sim$ 23 - 63 GeV) and 546 GeV. Fig. 5 shows CDF 1.8 TeV data (preliminary) and UA5 data at 546 GeV, where the charged particles are counted in progressively shorter ranges of η. The KNO distribution broadens substantially for smaller η ranges, perhaps reflecting larger statistical fluctuations due to smaller track samples per event. The distributions are very similar at the two energies. The 1.8 TeV data use uncorrected charged particle multiplicities. The systematics of high multiplicity events are still under study, and the inefficiencies could be relatively large.

6. TRANSVERSE MOMENTUM DISTRIBUTIONS AND $< p_T >$

Since this talk was presented, these results have appeared in print[13], to which the reader is referred for details of the analysis and for some of the figures. The CTC has >99% efficiency for tracks with $p_T > 400$ MeV/c and $|\eta| < 1$. The charged particle invariant cross section is defined as:

$$Ed^3\sigma/d^3p = (\sigma_{eff}/N_{evt})(N/p_T \cdot \Delta p_T \cdot \Delta\phi \cdot \Delta y)$$

where N_{evt} is the number of events used and N is the number of charged tracks in a given element of phase space. The invariant cross section as a function of p_T for the CDF 630 GeV data (which extends only to 3.5 GeV/c) is in good agreement with the UA1 and UA2 data at 546 GeV. The CDF data at 1.8 TeV extend to $p_T = 10$ GeV/c, and fall less rapidly with p_T than the 630 GeV data[13], being a factor of 4 higher at 3.5 GeV/c. Invariant cross sections were fitted to a parton-model-inspired power law

$$Ed^3\sigma/d^3p = A\frac{p_o^n}{(p_T + p_o)^n}$$

The parameters p_o and n are highly correlated and good fits can be obtained with a change in n compensating a change in p_o. We fix $p_o = 1.3$ GeV/c as is done at lower $\sqrt{s}$. (When

p_o is left free, the fit at 1.8 TeV gives $p_o = 1.29$)[13]. Values of n decrease as the spectra harden with increasing s:

detector	$\sqrt{s}$	n
UA1	546 GeV	9.14±.02
CDF	630 GeV	8.89±.06
CDF	1.8 TeV	8.28±.02.

Fig. 5 shows the CDF 1.8 TeV data, together with the UA1 data, ISR data (British Scandinavian) and Fermilab fixed target data (Chicago Princeton).[13] The 1.8 TeV data fall much less steeply with p_T, being 5 orders of magnitude larger than the 27 GeV data at p_T = 7 GeV/c.
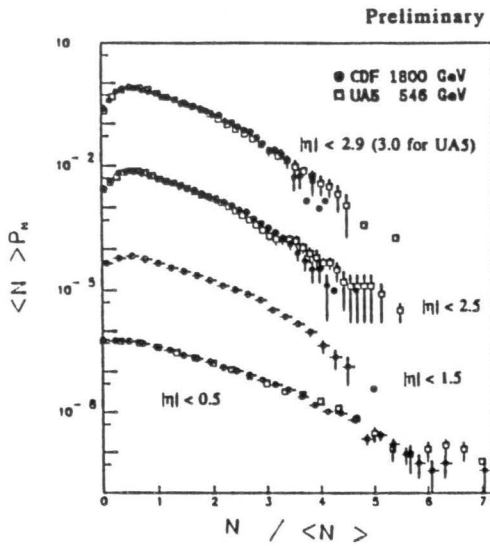
Fig. 4 $<N> P_N$ vs. $N/<N_>$, KNO distributions for CDF 1.8 TeV data and UA5 546 GeV data.
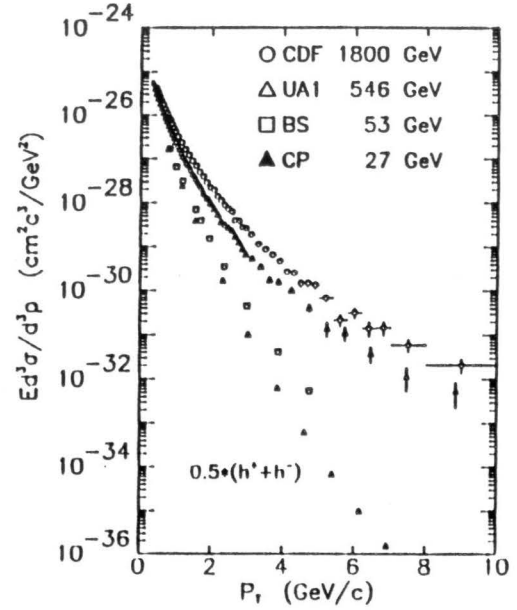
Fig. 5 Charged particle $(h^+ + h^-)/2$ invariant cross section vs. p_T.

A calculation by S. Ellis and J. Stirling[14], based on the parton model and QCD, attempts to predict the above data. The ingredients are (a) structure functions $F(x,Q^2)$ for two colliding partons, one in the proton and one in the anti-proton determined from experiment and from QCD evolution in Feynman x, (b) fragmentation functions $D(z)$ for production of various hadrons, again determined from experiment, and (c) a QCD parton-parton scattering cross section $\hat{\sigma}$ $(\hat{s}, \hat{t}, \hat{u})$. Fig. 6 shows the results of the calculations, using Duke and Owens set 1 structure functions with $Q^2 = p_T^2$ and a K-factor of 2. Compared with the data of Fig. 5 above $p_T = 1$ GeV/c, the p_T and s dependences agree, within a factor of ~ 2 to 5, over nine decades of invariant cross section.

In determining $< p_T >$, extrapolation is required for the substantial portion of the p_T

spectrum below the 400 MeV/c cutoff. Alternative functional forms used include: (a) the above power law form, (b) a simple exponential $A \exp(-bp_T)$ and (c) a polynomial $A(p_T^2 + B.p_T + C)$. Systematic uncertainties due to choice of functional form are much reduced by the powerful constraint that the area under the entire curve must be given by $dN/d\eta$. When the three functions are fitted to the data between 400 and 600 MeV/c, (Fig. 7) with $dN/d\eta$ fixed, the systematic error in the extrapolation is reduced to 0.003 GeV/c. We use the well determined ratio $1.27 \pm .04$ of the plateau heights at 1.8 and 0.63 TeV (from Section 5), and fix $dN/d\eta = 3.30 \pm 0.15$ at 630 GeV by interpolating measurements in the range 200 to 900 GeV[9]. We then obtain $< p_T > = 0.495 \pm 0.014$ (0.432 ± 0.004) GeV/c at 1.8 (0.63) TeV. There is an additional common uncertainty of 0.020 GeV/c on both numbers due to the 5% uncertainty on $dN/d\eta$ at 630 GeV. The C0 experiment at 1.8 TeV quotes $< p_T > = 0.47 \pm 0.01$[15]. This value and the CDF value at 1.8 TeV are in good statistical agreement.
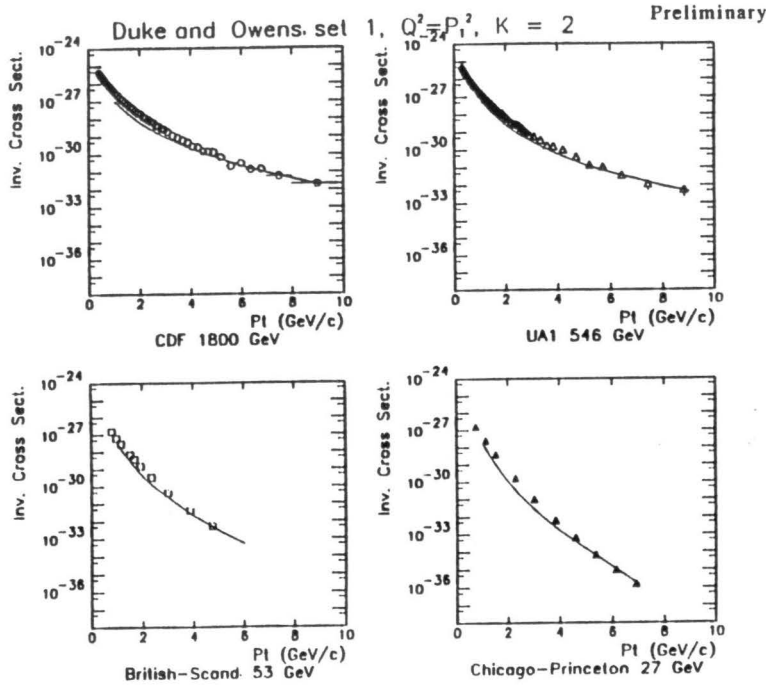

Fig. 6 Curves are a parton model calculation of Ellis and Stirling. Data are as in fig. 5.

Fig. 7 Curves are (left to right) functional forms a, b, and c described in the text, used to extrapolate to p_T=0.
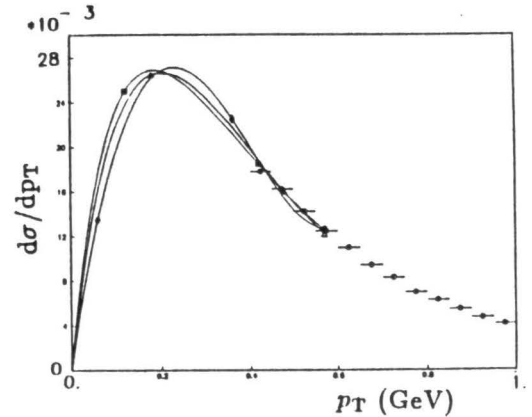
Fig. 8 shows $< p_T >$ as a function of s which rises substantially faster than ln(s). The common uncertainty of the two CDF points is omitted, and will not affect the steep slope from 0.63 to 1.8 TeV. The solid curve is a fit to the form $0.326 + 0.0044 \, s^{0.24}$, with $\chi^2 = 7.5$ for 9 degrees of freedom. The dashed curve is a fit to the form $0.433 - 0.025 \, \ln(s) + 0.0019 \, \ln^2(s)$, with $\chi^2 = 9.35$. Either curve describes the data well, and it is clear that a function linear in ln(s) would give a very poor fit.

Fig. 8 $< p_T >$ as a function of $\sqrt{s}$. The two curves are fits described in the text.

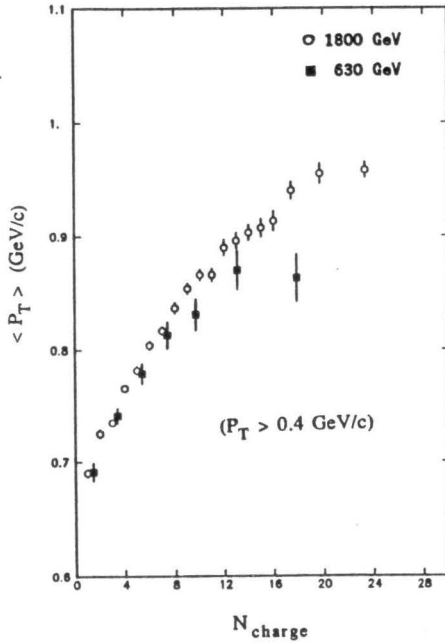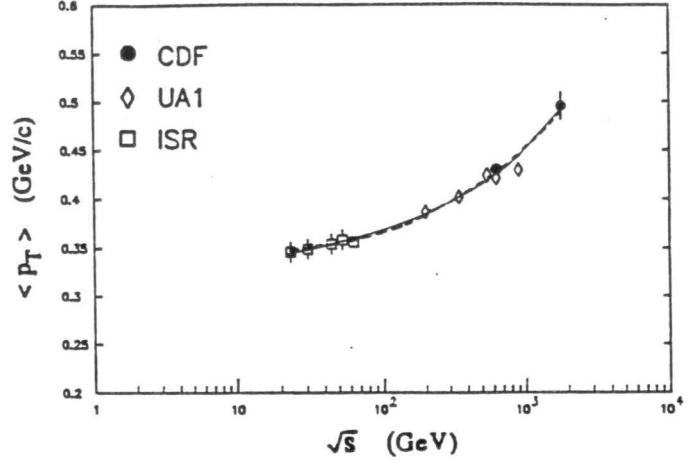Fig. 9 $< p_T >$ (calculated for $p_T > 0.4$ GeV) vs. N in the CTC. Data at 1.8 and 0.63 TeV.

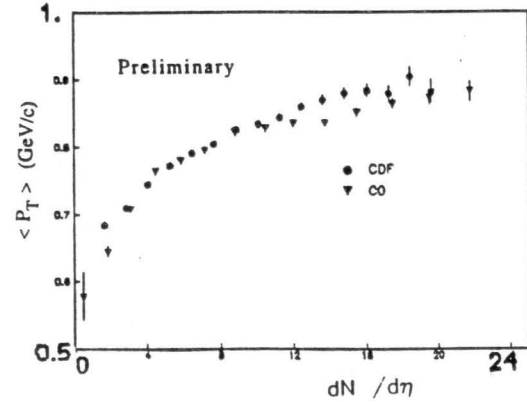Fig. 10 $< p_T >$ as a function of $dN/d\eta$ for CDF and C0 1.8 TeV data. $< p_T >$ are calculated for $0.4 < p_T < 3.0$ GeV).

We have determined $< p_T >$ for various ranges of charged particle multiplicity seen in the range $|\eta| < 1.0$ in the CTC (Fig. 9). The $dN/d\eta$ constraint is lost, and $< p_T >$ is averaged over the range of the data from 0.4 to 10 GeV/c, and no extrapolation is attempted. Within the statistical errors, the data are consistent with a smooth increase of $< p_T >$ with increasing N. There is no evidence for a phase transition as postulated for the Quark Gluon Plasma (QGP). However, in the absence of charged particle data below 400 MeV/c, conclusions pro or con the QGP are not warranted. The C0 experiment has data down to $p_T = 150$ MeV/c[15], and is complementary to CDF in the p_T range covered.. Fig. 10 compares CDF and C0 data at 1.8 TeV, where $< p_T >$ is averaged over the range $0.4 < p_T < 3.0$ GeV/c, common to both experiments. VTPC multiplicities for CDF are from $|\eta| < 2.5$ (caveats of Section 5 apply). C0 multiplicities are for $|\eta| < 3.25$. The data are in reasonable agreement, and have rather smooth variation with $dN/d\eta$.

7. K_s^0 DATA

Neutral strange particles decaying into 2 charged particles ("Vees") were studied using CTC tracks with momentum $p_T > 0.25$ GeV/c and having transverse impact parameter d ≥ 2 mm with respect to the primary event vertex. A geometrical fit to the Vee, with one degree of freedom, was accepted if the χ^2 was less than 5. The impact parameter of the Vee momentum vector was required to be: $D_{pair} < 2$ cm. To reduce background from primary charged particles, the Vee vertex was required to be at a radius R > 2 cm.

A search for K_s^0 in the 1.8 TeV data yielded 402 events above a background of 64 events, as seen in the $\pi^+\pi^-$ invariant mass plot (Fig. 11). A fit gives a mass M = 496.8 MeV/c^2, a mass resolution $\sigma_M = 9.2$ MeV/c^2, and an almost linear background (with a very small term quadratic in M), with $\chi^2 =$ for degrees of freedom. Events neighboring the K_s^0 mass peak, representing the background in the signal region, were subtracted for all K_s^0 distributions.

Acceptance and track- and Vee- finding efficiencies were determined by implantation into real events of Monte Carlo K_s^0, generated with full CDF detector simulaton. The overall efficiency, which was used to weight each event, is between 0.14 and 0.28 for p_T in the range 1.4 to 10 GeV/c. The efficiency becomes very small below 600 MeV/c, due to spiralling in the CTC of tracks below 330 MeV/c and due to the applied track momentum cut at 250 MeV/c. The K_s^0 efficiency has recently been found to depend on the charged particle multiplicity in the CTC. Extensive MC implantation studies are underway, and the results may substantially affect the K_s^0 distributions.
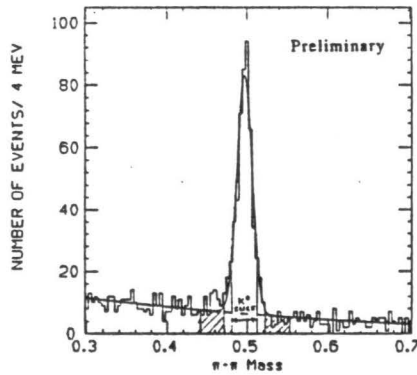

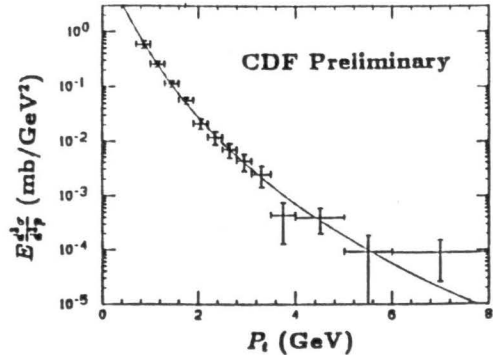Fig. 11 Vee$\rightarrow \pi^+\pi^-$ effective mass plot, with Gaussian fit to K_s^0, as described in text.

Fig. 12 K_s^0 invariant cross section as a function of p_T, for CDF 1.8 TeV data.

A preliminary K_s^0 invariant cross section as a function of p_T is shown in Fig. 12. It

was fitted over the range $0.7 \leq p_T \leq 8.0$ GeV/c, using a Poisson likelihood function, to the same power law form as for the charged hadron spectrum, again with $p_o = 1.3$ GeV/c. The exponent is found to be n = 7.49 $\pm$ 0.23. It is smaller than for the charged hadron data by Δn = 0.79 $\pm$ 0.23, corresponding to a ratio $K_s^0/h^{\pm}$ which rises with p_T. This preliminary value of n is consistent with values measured by UA5 at lower $\sqrt{s}$[16], for example n = 7.57 $\pm$ 0.39 at 900 GeV. It is also consistent with a continuing decrease of n as $\sqrt{s}$ increases [16], reflecting a continued hardening of the K^os p_T spectrum.

8. CHARGED PARTICLE CORRELATIONS

A tendency is seen for charged tracks to cluster in η and ϕ. The CTC track sample studied is restricted to $|\eta| < 1.0$. Fig. 13 shows the charged particle transverse momentum density around trigger particles having various ranges of p_T. The distributions exclude the p_T of the trigger particle. Fig. 13a shows $d\sigma_{p_T}/d\Delta\eta$ as a function of distance in pseudorapdity from the trigger particle, for "same-side" tracks having ϕ within 90° of the trigger particle. There is clear peaking around the trigger particle, which becomes more pronounced for larger trigger p_T. Fig. 13b shows a strong tendency for momentum density $d\sigma_{p_T}/d\Delta\phi$ to peak both in the direction of the trigger particle and also at $d\phi = 180°$ opposite to the trigger particle. Fig. 13c is for away-side tracks, in the ϕ semicircle opposite to the trigger particle. No η correlation is seen.
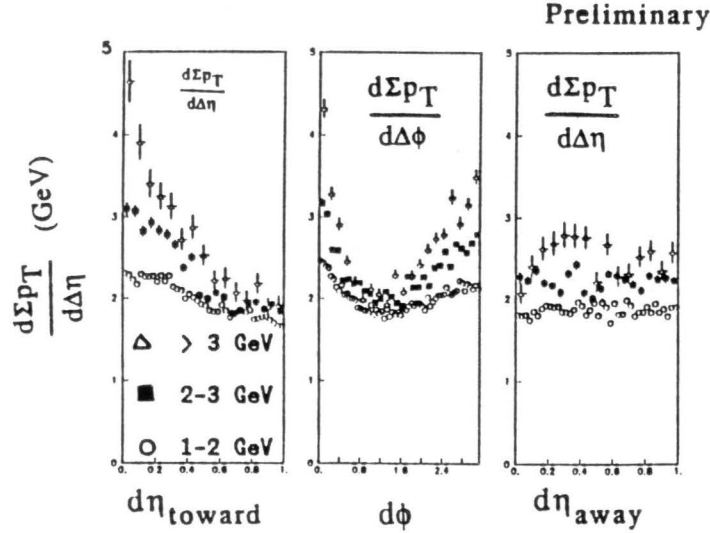

Fig. 13 Charged particle momentum densities around trigger particles of various p_T, for (a) same-side and (c) away-side particles as a function of distance in η from trigger particle; (b) as a function of distance in ϕ from trigger particle.

The same patterns are seen, but are much more pronounced, in a sample of jet events (not shown) which were selected using a central calorimeter jet trigger with 70 GeV threshold and which is dominated by two-jet events. The absence (presence) of away-side correlations in η (ϕ) can be understood in terms of parton-parton collisions with small overall p_T and conservation of p_T, and with a wide spread of overall longitudinal momentum, p_Z, reflecting the Feynman-x distributions of the colliding partons.

The patterns of Fig. 13 are consistent with the observation of the charged portion of low-p_T jets. This further motivates a search for charged clusters using an algorithm similar

10

to the calorimeter transverse energy E_T clustering algorithm used to find jets[5]. Using only charged tracks has certain advantages over calorimeter clustering for low p_T jets: (a) track momentum resolution σ_{p_T}/p_T is less than 2.5% for the MinBias event sample, (b) track directions at the primary vertex are used, whereas low momentum tracks are swept by the magnetic field to the wrong azimuth at the calorimeter, (c) the calorimeter response is known to be nonlinear at low E_T. Disadvantages of clustering charged tracks include: (a) on average, one-third or more of the hadronic energy is expected to be in neutral particles and (b) event-to-event fluctuations in the neutral to charged energy ratio will smear the jet energy estimate.

We use the CTC track sample with $|\eta| < 1.0$. A charged cluster is defined as a set of tracks within a cone of half-angle 40° around a common axis along the cluster momentum vector. Only tracks having rapidity $y > y_o = 2.0$ along the common cone axis are used. The search starts with the axis along the highest-p_T track, and iteratively adjusts the cone axis as the cluster is formed. Particles are used in descending p_T until up to 4 clusters are found. The cluster transverse energy is then calculated:

$$E_T^{clust} = [(\Sigma E_i)^2 - (\Sigma P_{zi})^2]^{1/2}$$

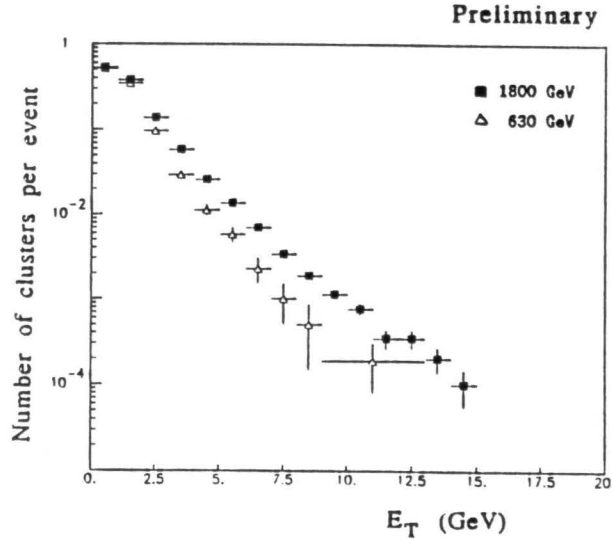where the E_i are calculated using the pion mass.

Fig. 14 E_T distribution of charged clusters
for CDF data at 1.8 TeV and 630 GeV.

The E_T^{clust} spectra for clusters with $|\eta| < 0.7$ are shown in Fig. 14 for 1.8 TeV and 630 GeV MinBias events. The spectrum is seen to harden as $\sqrt{s}$ increases, with a factor of 4 rise for $E_T^{clust} \sim 7$ to 10 GeV. These charged clusters occur quite copiously, with 35 to 40% probability per MinBias event for $1 \leq E_T^{clust} \leq 2$ GeV. At 1.8 TeV the integrated probability of a cluster with $E_T^{clust} > 3$ GeV is 11% per event, corresponding to a preliminary cross section of 4.7 mb in the central 1.4 units of η.

11

ACKNOWLEDGEMENTS

REFERENCES

1) F. Abe et al., Nucl. Inst. Meth. A271 (1988) 387.

2) G. Altarelli, K. Ellis, M. Greco, and G. Martinelli, Nucl. Phys. B246 (1984) 12;
   G. Altarelli, K. Ellis, and G. Martinelli, Z. Phys. C27 (1985) 617.

3) F. Abe et al., A Measurement of W Boson Production in 1.8 TeV $\bar{p}p$ Collisions, (submitted to Phys. Rev. Lett.).

4) E. Eichten, Theoretical Expectations at Collider Energies, Fermilab-Conf-85/178-T (Fermilab report, May, 1986) p. 92.

5) F. Abe et al., Measurement of the Inclusive Jet Cross Section at the Tevatron $\bar{p}p$ Collider, (submitted to Phys. Rev. Lett.).

6) F. Snider et al., Nucl. Inst. Meth. A268 (1988) 75.

7) F. Bedeschi et al., Nucl. Inst. Meth. A268 (1988) 50.

8) D. Bernard et al., Phys. Lett. 186B (1987) 227.

9) G. Ekspong, Nucl. Phys. A461 (1987) 145, and references therein.

10) Dual Parton Model, A. Capella, U. Sukhatme, C-I Tan, and J. Tran Thanh Van, Multiparticle Production, ed. P. Carruthers (World Scientific,1988); ratio is from a Monte Carlo program made available by J. Tran Thanh Van. For an extension of the DPM to include hard parton collisions, see J. Ranft et al., SSC Central Design Group report SSC-149 (December, 1987); ratio is from a Monte Carlo calculation by J. Ranft (private communication).

11) H-U Bengtsson and T. Sjostrand, Computer Phys. Communications 46 (1987) 43.

12) G. J. Alner et al., Phys. Lett. 138B (1984) 304,
    G. J. Alner et al., Phys. Lett. 160B (1984) 199.

13) F. Abe et al., Phys. Rev. Lett. 61 (1988) 1819.

14) S. Ellis and W. J. Stirling, private communication.

15) C. Lindsay, Recent Results from E-735: Search for Quark Gluon Plasma in $\bar{p}p$ Collisions at $\sqrt{s} = 1.8$ TeV, this volume.

16) R. Ansorge et al., Phys. Lett. B199 (1987) 311, and submitted to Zeit. Phys. C.